Photogrammetric Record, 17(9#): 000–000 (April / October 200#)

METRIC CAPABILITIES OF LOW-COST DIGITAL CAMERAS FOR CLOSE RANGE SURFACE MEASUREMENT

By JIM H. CHANDLER (j.h.chandler@lboro.ac.uk),
Loughborough University, UK

JOHN G. FRYER (john.fryer@newcastle.edu.au),
University of Newcastle, Australia

and AMANDA JACK (a.jack@sir-robert-mcalpine.com)
Sir Robert M^{c}Alpine Ltd, Hemel Hempstead, UK

Abstract

This paper examines the potential of low cost digital cameras for close-range surface measurement using feature based image matching methods. This is achieved through extracting digital elevation models (DEMs) and comparing accuracies between three low-cost consumer grade digital cameras (Sony DSC-P10, Olympus C3030, Nikon Coolpix 3100) and the proven Kodak DCS460. Surprisingly, the tests revealed that the highest accuracies were achieved using the Sony DSC-P10, not the Kodak DCS460, whilst the other two cameras certainly proved suitable for most close-range surface measurement tasks. Lens modelling was found to provide a limiting constraint on final accuracies, with very small systematic error surfaces caused by residual imperfections in lens modelling. The IMAGINE OrthoBASE Pro software and an independent self-calibrating bundle adjustment were used to process these data. These tests identified an inaccuracy in the self-calibrating capability of IMAGINE OrthoBASE Pro version 8.6 and Leica Geosystems LPS 8.7, which will be rectified in subsequent software releases. The study has demonstrated that cheaper consumer grade digital cameras have potential for routine surface measurement provided lens modelling is considered. The lead author is maintaining a web based repository for camera calibration data, which may assist other users.

KEYWORDS: close range photogrammetry, DEM extraction, digital cameras, surface measurement

INTRODUCTION

Digital camera technology is becoming cheaper, mainly due to exploitation of the mass consumer market where new ranges of digital cameras are becoming available at an increasing rate. A significant consequence is that sensor resolution is increasing rapidly, with new ranges of 3 to 5 Mega-pixel cameras being readily affordable (US$300-400) for both the layperson and the scientist. The resolution of the high end of this new generation of digital cameras is such that it rivals that available from traditional 35mm film-based cameras. This paper explores the use of these digital cameras for the measurement of surfaces at close range.

The ability to measure and record surfaces is important to many scientific disciplines and both photogrammetry and laser scanning provide the required capability. Laser scanning remains expensive, is only just portable and the inbuilt camera/video system, which is an integral part of the aiming system, is usually not of sufficient resolution to provide high quality image information; although this shortcoming will undoubtedly change in the near future. Such image information is essential for interpretation, particularly within regions of surface homogeneity where surface morphology alone is unable to convey location. Photogrammetry provides many advantages for surface measurement, potentially creating both image and morphological information, but has suffered because of the financial costs associated with the necessary software, the need to develop appropriate expertise, and until recently, the cost of digital sensors of adequate resolution and geometric fidelity. In this study, a selection of inexpensive digital cameras is compared with the photogrammetrically proven digital sensor of the recent past, the Kodak DCS460, with some surprising results.

SURFACE MEASUREMENT

There are many scientific and medical disciplines which need to derive accurate surface representations. Diverse scientific applications include the work of the field archaeologist who needs to rapidly record and measure exposed artefacts (Ogleby et al., 1999; Desmond and Bryan, 2003; Fryer, 2001; El-Hakim et al., 2004); geomorphologists who need to measure natural terrain surfaces undergoing morphological changes driven by earth surface processes, including fluvial (Stojic, et al., 1998; Lane et al., 2000; Lawless and Robert, 2001, Hancock and Willgoose, 2001; Chandler et al., 2003) and landslide dynamics (Chandler and Brunsden, 1995; Walstra et al., 2004). In civil engineering those involved in developing computational fluid dynamics often need to measure dynamic and mobile surfaces created by physical experiments (Chandler at al, 2001) to verify numerical models. Finally, in the medical sciences Mitchell and Newton (2002) review and identify how photogrammetry has been used to measure body surfaces, including deformation of the spine (scoliosis) and tooth decay.

Techniques to enable the use of cheap non-metric cameras for spatial measurement have become well established, with many notable contributions during development of analytical photogrammetric methods in the 1970s and 80s.

Abdel-Aziz & Karara (1971) developed the DLT method, which bypassed the requirement of fiducial marks. Work conducted by Brown (1972), Kenefick et al, (1972) and Faig (1975) developed sophisticated mathematical models to represent the deviation from perfect collinearity occurring within non-metric cameras. Hottier (1976) undertook experiments to assess the accuracy of a range of lower-priced cameras including the Hasselblad 500 (US$550 in 1976) and the very cheap Kodak Instamatic 154 (US$15 in 1976). He reports that sophisticated distortion models are not required and that a simple single radial lens parameter (kr^3) is appropriate and that other refinements seem to be unnecessary. The Kodak DCS460 and its predecessors (DCS420/DCS200) have received widespread attention for photogrammetric measurement (Fraser and Shortis, 1995; Ganci and Shortis, 1996; Fraser, 1997) but cheaper sensors and competition have provided new opportunities. Most recently, Cardenal et al., (2004) describes the use of the 3.2 Megapixel Canon D30 for photogrammetric recording of historical buildings. It is stated that this particular camera is effective at low/medium precision for archaeological and architectural studies. Ogleby (2004) glimpses into the future and predicts the "Ridjidigital", a combined Terra-pixel imaging and laser scanning device with limitless storage, ideally suited for heritage documentation; but what do current and cheap consumer grade digital sensors have to offer now?

THE STUDY

Initial experiment- Kodak DCS460

The impetus for the initial study was to guide a Masters student through a final year project. Previous activities by the lead author had involved investigating the accuracies of the ERDAS IMAGINE OrthoMAX automated digital elevation model (DEM) extraction software (Gooch & Chandler, 1998), which uses an area-based correlation method. It appeared that this field could again yield a fruitful topic, simply by updating the approach using the latest software tools provided by OrthoBASE Pro, which instigates a feature based matching method for DEM generation (ERDAS, 2002).

In previous studies it had proved difficult to generate reliable accuracy statistics from the comparatively limited number of checkpoints that could be practicably provided. An alternative was to design a test object of simple geometry that could provide thousands of checkpoints and allow the accuracy of the automated DEM extraction software to be assessed with statistical reliability. A flat and planar surface was provided by a piece of 0.8 x 0.6 m medium-density fibreboard (MDF) to which two square blocks of smooth MDF were added (Figure 1). These blocks were 47 and 100 mm in height and attempted to replicate physical structures such as buildings found in the real world. A third sloping block with a maximum height of 47 mm was added also, to provide a more challenging structure for the software to measure automatically. The MDF board and blocks were sprayed with white paint and finally splattered with thinned red and blue paint (Figure 1). This was done to provide an appropriate texture for the image

matching algorithm embedded in the OrthoBASE Pro software to correlate reliably.

[Figure 1 about here]

Twelve photogrammetric targets were distributed over the board, including the four corners of the MDF and the upper corners of the simulated building blocks. These targets were purchased from a commercial supplier, were 10 mm in diameter and of conventional black and white design. A theodolite intersection method was used to coordinate each of these targeted points. Both horizontal and vertical angles were measured using a Leica TC1010 total station, with horizontal distances measured between the two theodolite stations and a subset of the photogrammetric targets using a steel band. Initial coordinate estimates for the targeted points were computed using basic intersection formulae but eventually all measurements were combined in a unified least squares procedure to derive the best estimates for the targeted points (3D precision: 0.9 mm). These coordinates were used for two further purposes: to provide conventional control for the photogrammetry; and, to generate the accepted three dimensional geometry of the test object. This geometry was initially represented by a series of three dimensional coordinates delineating the corners and edges of the blocks and the flat MDF surface. These coordinates were used to create a DEM at 1 mm resolution, known as the "truth DEM" (Figure 2), which could be compared with the photogrammetrically derived representations.

[Figure 2 about here]

For the initial project, imagery of the test subject was acquired using a Kodak DCS460 equipped with a 24 mm lens. This camera was originally launched in March 1995 and has proven photogrammetric capability (Fraser, 1997; Shortis et al., 1998; Chandler et al., 2001). A simple convergent stereopair was acquired from a distance of 0.9 m and camera separation of 0.16 m. This represented a base to distance ratio of 1:6 and could be regarded as typical for the type of basic three dimensional measurement of surfaces that many scientists would conduct. Before accurate data could be extracted, it was necessary to establish an appropriate transformation between image and object, or restitution, which for non-metric imagery requires appropriate definition of both internal and external orientation parameters. For the student project, an accurate inner camera model was provided through the use of an external "in-situ" self calibrating bundle adjustment, (Kenefick et al., 1972; Atkinson, 1996) known as GAP (Chandler and Clark, 1992). Once a satisfactory restitution had been achieved, a variety of DEMs were extracted using OrthoBASE Pro with differing strategy parameters. The DEMs were extracted at 3 mm resolution and were compared with the truth DEM by interpolation and subtraction. An ERDAS graphical model was developed to derive mean error and standard deviation of error, as recommended by Li (1988). Accuracy assessments based upon this approach are more informative than the ubiquitous root mean square error as both systematic (reflected in the mean error or bias) and random effects (standard deviation) are differentiated.

It became obvious that the methodology adopted provided a very quick and easy way to assess the metric capability of any camera for simple surface measurement. Imagery could be acquired in five minutes and within an hour, DEMs could be generated and accuracy assessed. A further series of images of the test object was then collected using digital cameras that were both cheaper and more widely available.

Main tests- Sony DSC-P10, Olympus C3030, Nikon Coolpix 3100

Three other cameras have been tested to date, these are: Sony DSC-P10, Olympus C3030 and the Nikon Coolpix 3100. All three cameras are readily available at prices below US$400 (August 2004). They are equipped with variable zoom lenses and have small CCD arrays when compared to the DCS460, which has an active image area that physically matches a conventional 35mm film camera (Table 1). The reduced image areas of the cheaper sensors require shorter focal lengths (Table 1) to achieve similar object coverage but are normally marketed with focal lengths which are 35mm format equivalents.

Sensor	*Sensor size (mm)*	*Resolution (pixels)*	*Pixel size (μm)*	*Focal length and 35mm equivalent (mm)*
Kodak DCS460	*27.6 x 18.6*	*3060 x 2036*	*9.02 x 9.14*	*24.9/24.9*
Sony DSC-P10	*7.18 x 5.32*	*2592 x 1944*	*2.77 x 2.74*	*7.8/38*
Olympus C3030	*7.18 x 5.32*	*2048 x 1536*	*3.51 x 3.46*	*5.8/35*
Nikon Coolpix 3100	*5.27 x 3.96*	*2048 x 1536*	*2.57 x 2.58*	*5.8/38*

Table 1- Sensor parameters

Basic stereo images with a Base/Distance ratio of approximately 1:6 were acquired with all three cameras, with an additional third image acquired midway between the pair. A similar camera/object distance of approximately 0.9 m was maintained, although some variation was inevitable. The overriding desire was to utilise the full format of the image using the wide angle view setting and although differing image scales were achieved, the area covered by each pixel on the plane defined by the MDF board was broadly similar for all sensors, (Table 2). Images were stored on internal memory cards using the "high quality" JPEG storage

Sensor	***Camera Height (m)***	***Approx Image scale***	***Pixel size on MDF plane (mm)***	***JPEG Compression ratio***
Kodak DCS460	*0.90*	*1:36*	*0.32*	*None*
Sony DSC-P10	*0.90*	*1:115*	*0.32*	*1:2.2*
Olympus C3030	*0.64*	*1:110*	*0.38*	*1:1.9*
Nikon Coolpix 3100	*0.83*	*1:143*	*0.37*	*1:1.8*

Table 2- Acquired image and pixel geometry achieved during main tests

option provided, and Table 2 indicates the compression ratios actually used. The stereo imagery was used in OrthoBASE Pro as 8-bit greyscale, whilst the centre frame was stored in full 24-bit colour. This combination was justified because OrthoBASE Pro's automated DEM extraction only uses a single colour band, whilst the central image was intended for full colour orthophoto production.

Camera calibration

The www.dpreview.com website was used to ascertain the physical dimensions of the sensors and their resolutions (e.g. Nikon 3100: dpreview, 2004). This data was used to ascertain the physical size of each pixel in the X and Y directions (Table 1), an essential requirement for initial definition of primary inner orientation of the sensors in OrthoBASE Pro. Once image pyramid layers had been generated, the point measurement tool was used to measure each target manually, before 80 tie points were added automatically. The OrthoBASE triangulation algorithm, which implements a standard bundle adjustment, was then activated. This yielded the first of the calibration options tested in the study, entitled the "no lens model".

Four camera calibration options were investigated in total:

- The simplest or "no lens model" refers to the most basic calibration option in which only an approximate focal length was utilised and radial and de-centring lens distortions were completely ignored. With the type of non-metric cameras used, poor results were expected.
- The second calibration option entitled "OrthoBASE self-calibration" utilised the inbuilt self-calibrating capabilities of OrthoBASE Pro, which implements a "14 parameter Brown model" (ERDAS, 2002) to compensate for most of the linear and non-linear forms of film and lens distortion. This model is a simplified version of the 29 parameters identified by Zhizhuo, (1990) and attributed to Brown (1972). ERDAS have reduced these to fourteen parameters felt most significant (Wang, 2004) and this model should, ideally, provide most users with the capability to calibrate non-metric cameras.
- The third option utilised an external self-calibrating bundle adjustment known as GAP (Chandler and Clark, 1992). This uses three parameters to model the primary inner orientation (focal length, and x_0, y_0 displacements of the principal point), three parameters to model radial lens distortion and two for decentring distortion (Kenefick et al., 1972; Chandler and Clark, 1992). The other optional parameters include terms for affinity and non-orthogonality of the photo coordinate axes (Patias and Streilein, 1996). Once a satisfactory estimation had been obtained, the derived inner orientation parameters were re-established into OrthoBASE Pro by direct entry of the focal length and principal point offsets. The radial lens model was recreated by entering radial distortions at increasing radial distances and then recomputing the lens parameters required by OrthoBASE Pro.
- The fourth and final approach was a hybrid of the second and third calibration options. The lens model was provided by external self-calibration provided by

GAP but the primary inner orientation (focal length, and x_0, y_0 displacements) was estimated by OrthoBASE Pro.

DEM generation

OrthoBASE Pro uses a hierarchical feature based matching algorithm that incorporates both pyramid image layers and an epipolar constraint to reduce the search time for conjugate points in image pairs. The basic approach of creating DEMs in OrthoBASE Pro and then estimating accuracies by comparing elevations with the truth DEM was replicated, although with two significant modifications. To avoid the introduction of too many variables into the study, the "default" strategy parameters controlling DEM generation were used throughout. These use a "Search Size" in X and Y of 21 and 3 pixels respectively; a "Correlation Size" (template) of 7 x 7 pixels; and, a Correlation Coefficient Limit of 0.8 as a threshold to identify a successful match in the imagery. OrthoBASE Pro is able to alter these three parameters dynamically during DEM generation but for simplicity all such "adaptive capabilities" were switched off. The DEMs created for each camera represented the whole of the physical test object and were therefore entitled "full area DEMs". During these tests it was apparent that the accuracy statistics were distorted by areas of failure around the tops and bottoms of the wooden blocks. This effect was entirely predictable and arises due to the perspective of the cameras creating the well known "dead ground effect" (Skarlatos, 1999) causing poor height estimates due to inappropriate interpolation. In order to isolate and remove these gross errors, a smaller DEM representing the central and flat part of the test object was created for each camera, known as the "central area DEM". This avoided the physical blocks completely and enabled the optimum accuracies for each camera to be quantified.

RESULTS

Camera calibration

Table 3 summarises the calibration results generated by using the four different calibration approaches for the four different cameras. The first three columns represent RMS Error (mm) in the object space, whilst the final four columns tabulate the RMS Error residuals in the image space (μm and pixels). As would be expected, it is immediately apparent that some form of camera calibration is essential for accurate restitution for all four cameras, with the hybrid calibration approach producing the optimum results. This was achieved by using an external calibration to derive a lens distortion model and OrthoBase self-calibration to derive focal length and principal point offset. What is disappointing is that this could not be achieved using the OrthoBase self-calibration routines alone. The calibration achieved using just GAP, generated results that were almost as accurate as the hybrid approach, the latter providing only marginal improvement.

Camera/calibration option	Object RMS Errors (mm)			Image RMS Errors (μm)		Image RMS Errors (pixels)	
	X	*Y*	*Z*	*x*	*y*	*x*	*y*
Kodak DCS460							
No lens model	*1.7*	*0.8*	*3.6*	*2.4*	*3.2*	*0.27*	*0.35*
Obase Professional	*0.5*	*0.3*	*2.8*	*2.1*	*3.0*	*0.23*	*0.33*
GAP (f, k_1, k_2)	*0.3*	*0.2*	*0.3*	*1.7*	*1.7*	*0.19*	*0.18*
GAP + Obase Pro.	*0.2*	*0.1*	*0.2*	*1.8*	*1.6*	*0.18*	*0.17 †*
Sony DSC-P10							
No lens model	*2.9*	*2.2*	*2.3*	*2.3*	*1.2*	*0.82*	*0.42*
Obase Professional	*2.9*	*2.2*	*2.3*	*2.3*	*1.2*	*0.82*	*0.42*
GAP (f, k_1, k_2)	*0.9*	*1.3*	*0.4*	*0.4*	*0.7*	*0.16*	*0.25*
GAP + Obase Pro.	*0.9*	*1.3*	*0.3*	*0.4*	*0.6*	*0.14*	*0.22 †*
Olympus C3030							
No lens model	*3.5*	*2.3*	*2.7*	*1.0*	*1.4*	*0.28*	*0.40*
Obase Professional	*2.7*	*1.8*	*1.5*	*0.7*	*1.3*	*0.20*	*0.38*
GAP (f, k_1, k_2)	*1.0*	*1.5*	*0.6*	*0.6*	*0.6*	*0.16*	*0.17*
GAP + Obase Pro.	*0.9*	*1.4*	*0.4*	*0.4*	*0.6*	*0.11*	*0.17 †*
Nikon Coolpix 3100							
No lens model	*2.8*	*1.6*	*4.0*	*0.6*	*0.8*	*0.31*	*0.31*
Obase Professional	*2.8*	*1.6*	*4.0*	*0.7*	*0.8*	*0.27*	*0.31*
GAP (f, k_1)	*0.8*	*0.5*	*0.5*	*0.6*	*0.6*	*0.21*	*0.23*
GAP + Obase Pro.	*0.5*	*0.5*	*0.3*	*0.5*	*0.6*	*0.19*	*0.22 †*

† indicates calibration option which generates the minimum or optimum RMS error

Table 3- Calibration accuracies
("Obase Professional" figures revised in Table 5 using updated LPS, version 8.8)

In terms of accuracy of fit to the control points by camera, the optimum accuracies were achieved using the Kodak DCS460 (average RMS error 0.2mm) but the other cameras achieved sub-millimetre accuracy also, if appropriate camera calibration was performed. The performance of the Nikon Coolpix was particularly encouraging, achieving an average RMS error of 0.4 mm in the object space.

In the image space, accuracies varied between 0.4 to 1.7 μm, with the Kodak DCS460 performing worst. However, taking into account sensor size and expressing these rms errors in pixel units (Table 3) it is notable that there is a high degree of consistency between all cameras of approximately 0.2 pixels. This certainly indicates satisfactory conformance to image ray modelling at the selected image measurement precision but implies also that these sensors have similar metric potential once lens modelling and primary inner orientation have been considered.

DEM generation

Table 4 summarises the accuracy of DEM generation generated by using the four different calibration approaches for the four different cameras within the two areas tested - the full area occupied by the test object and the reduced central area which did not include the wooden blocks.

It is again apparent how important an appropriate camera calibration is for extracting accurate DEMs. For all four cameras, very poor DEM accuracies were achieved if no calibration was performed. Although expected, it was disappointing

Camera/calibration option	DEM accuracy- Full area *Mean and std. dev (mm)*	DEM accuracy- Central area *Mean and std. dev (mm)*
Kodak DCS460		
No lens model	*-5.5 ±7.4*	*-7.4 ±1.6*
Obase Professional	*-3.8 ±7.2*	*-5.6 ±1.6*
GAP (f, k_1, k_2)	*-0.6 ±9.5 †*	*-0.1 ±0.4 †**
GAP + Obase Pro.	*-0.7 ±9.0 **	*-0.4 ±0.4*
Sony DSC-P10		
No lens model	*-6.0 ±8.7*	*-8.3 ±1.4*
Obase Professional	*-3.9 ±7.8*	*-4.6 ±1.0*
GAP (f, k_1, k_2)	*-0.2 ±6.1 †**	*-0.1 ±0.3*
GAP + Obase Pro.	*-0.5 ±6.1*	*-0.0 ±0.3 †**
Olympus C3030		
No lens model	*-3.4 ±8.7*	*-5.5 ±1.8*
Obase Professional	*-0.6 ±8.7*	*-2.6 ±1.8*
GAP (f, k_1, k_2)	*-0.3 ±7.8 †**	*+0.2 ±0.5 †**
GAP + Obase Pro.	*-1.1 ±7.8*	*+1.4 ±0.7*
Nikon Coolpix 3100		
No lens model	*-6.1 ±8.3*	*-8.3 ±1.4*
Obase Professional	*+5.3 ±10.6*	*-8.0 ±1.3*
GAP (f, k_1)	*-0.8±6.7 **	*-1.0 ±0.4*
GAP + Obase Pro.	*-0.1 ±7.8 †*	*-0.4 ±0.4 †**

† indicates calibration option which generates the minimum or optimum mean error
** indicates calibration which generates the minimum or optimum standard deviation*

Table 4- DEM accuracies (mean error and standard deviation of error)

to see that the inaccurate restitution achieved using OrthoBASE self-calibration was reflected in all DEMs generated by all cameras. Optimum results were achieved using either GAP or the hybrid calibration approach, depending whether the mean or minimum standard deviation is regarded as the prime accuracy statistic.

DEMs generated for the full test object do not yield accuracy statistics as promising as those achieved for the central test area. This smaller area does not include the wooden blocks and consequently accuracy statistics are not affected by the small number of large failures for points adjacent to the blocks. More surprisingly, accuracies achieved using differing cameras did not follow expectations. The optimum accuracy for the central area combined with the hybrid calibration was not achieved using the proven, more complex and expensive Kodak DCS460 (-0.1 ±0.4 mm) but the Sony DSC-P10 (-0.0 ±0.3 mm). The Sony DSC-P10 is equipped with a 5 Mega-pixel sensor, only slightly lower than the 6 Mega-pixel Kodak DCS460 but being a compact camera with a variable zoom lens is approximately 11 times cheaper than a Kodak DCS Pro 14n, perhaps the current equivalent of the older DCS460. Resolution and camera type had limited effect on the accuracy of resulting DEMs, with the 3 Mega-pixel Nikon and Olympus cameras proving only slightly inferior to the 5 Mega-pixel Sony and 6 Mega-pixel Kodak cameras.

DISCUSSION

Camera calibration - number of lens parameters

During the derivation of an appropriate radial lens model using the external self-calibrating bundle adjustment GAP it was not obvious whether one or two radial parameters would be required. Normal practice requires the derived parameter to be compared with its estimated standard deviation and, if lower, it should be removed from the estimation. In most of the camera calibrations (Table 1) the second parameter (k_2) was marginally significant and estimated. However, for the Nikon Coolpix just a single radial lens parameter was recovered. Figure 3 represents the radial distortion curve estimated for the Nikon with either just the k_1 or both the k_1 and k_2 parameters estimated. Initial inspection suggests that the two curves appear distinct until it is realised that the absolute maximum radial distance for this particular sensor is just 3.3 mm. The two distortion curves are virtually indistinguishable between radial distances of zero and 3 mm. The differences never exceed 6 μm and even these values are achieved at radial distances rarely used for measurement. Both approaches create similar distortion curves and it is suggested that either calibration option would be acceptable. This confirms the work of Hottier (1978) and past experiences of the second author, which suggest that only one radial lens parameter is appropriate for the simple lenses employed by consumer grade cameras.

[Figure 3 about here]

OrthoBASE Pro self-calibration

The results achieved using the OrthoBASE Pro self-calibration routines alone (Table 3) were unsatisfactory, implying that there were functional difficulties with the OrthoBASE software. All tests were originally carried out using OrthoBASE Pro Version 8.6 although identical results were achieved using the latest product, (August 2004) where the self-calibration capability has become integrated within LPS 8.7.

The software manufacturer Leica Geo-systems was contacted and presented with the results summarised in Table 3. It was particular gratifying to receive a response within five days that confirmed the presence of an error in the software, which incorrectly evaluated root mean square errors for image coordinates. A replacement dynamic link library was subsequently provided for LPS 8.7 which included a new self-calibrating option to allow estimation of two radial lens parameters. This option was combined with estimation of the focal length and principal point offset and tested for the four cameras, yielding the revised calibration values in Table 5. These results replace the corresponding figures for "*Obase Professional*" conveyed in Table 3.

Camera	Object RMS Errors (mm)			Image RMS Errors (μm)		Image RMS Errors (pixels)	
	X	*Y*	*Z*	*x*	*y*	*x*	*y*
Kodak DCS460	*0.2*	*0.1*	*0.2*	*1.7*	*1.6*	*0.19*	*0.17*
Sony DSC-P10	*0.8*	*1.3*	*0.5*	*0.4*	*0.7*	*0.16*	*0.25*
Olympus C3030	*0.8*	*1.3*	*0.6*	*0.5*	*0.5*	*0.14*	*0.14*
Nikon Coolpix 3100	*0.4*	*0.4*	*0.3*	*0.5*	*0.6*	*0.19*	*0.22*

Table 5- Revised calibration accuracies for just the OrthoBASE Professional results originally conveyed in Table 3

It is gratifying that these results are virtually identical to those achieved using GAP and the hybrid calibration approach. It is hoped that this software correction and addition of the two parameter radial lens model should obviate the need to use an external camera calibration program in all future software releases, including LPS 8.8.

DEM generation

Figures 4 to 7 represent DEMs of difference for the full test object acquired using all four cameras and the GAP calibration solution. Solid red areas indicate elevations which are less than -5 mm, solid green regions indicate height differences greater than +5 mm, whilst white areas are indicative of no height differences between the "truth DEM" and automatically generated DEM data. It is striking that in the near vicinity of the wooden blocks significant areas of inaccurate DEM clearly illustrate the shadowing effect created by the blocks. If these regions are excluded from numerical analysis then DEM accuracies are typically better than 0.2 mm, with the Nikon generating the least favourable results (0.4 mm).

[Figures 4-7 about here]

The other obvious pattern exhibited by these difference images are the distinctive radial "domes" which appear to be approximately centred on each DEM. These are indicative of residual systematic effects in the DEMs arising from slightly inaccurate radial lens distortion parameters. Such domed structures have been noted in past work (Stojic et al., 1998; Chandler, et al., 2003) and a theoretical proof explaining them was given in Fryer and Mitchell (1987). This confirms that any uncorrected radial distortion introduces x-parallax into the stereomodel in the form of a cubic surface centred on the photo-base. It is suggested that the methodology adopted here, which has involved comparing over 350 000 measured elevations with their known values, has been particularly advantageous in their detection.

Consumer grade digital cameras have one significant advantage for surface measurement, the small sensor size. This may seem paradoxical, but the small sensor and consequent short focal length simplifies lens modelling considerably. Once the camera object distance is less than "a few tens of focal lengths of the camera" (Brown, 1972), varying lens models are strictly required for differing focus distances according to the Magill formula (Fryer and Mitchell, 1987). All of the consumer grade sensors were tested at camera object distances well above this

threshold. In contrast, the DCS460 camera was far closer to it and this possibly accounts for the reduced accuracy compared to the smaller Sony sensor.

Camera calibration data for accurate surface measurement

The camera calibration data files generated and used successfully in this project have been made freely available on a web site (http://snap.lut.ac.uk/Jim/Calibration/). The information is stored in the form of an OrthoBASE/LPS camera file, which can be loaded directly into these two software packages. The primary information includes a radial lens distortion model that strictly relates to a plane at a fixed distance from the camera and is associated with the calibrated focal length defined in the calibration file. However, this should serve as a first approximation for a variety of other focal length settings.

The methodology used to obtain camera calibration data suitable for close range surface measurement has proved efficient and effective. The first named author is therefore willing to test and calibrate other digital cameras using this particular approach and is hoping to extend the size of this freely available repository.

CONCLUSION

A series of tests have demonstrated that consumer-grade digital cameras are capable of generating DEMs to sub-millimetre accuracies at a camera-to-object distance of 1m. These accuracies are comparable with the proven Kodak DCS460 and the result implies that many other scientists could make use of cheap sensors for routine measurement of textured services using commercial photogrammetric software. Resolution remains important and it is perhaps prudent to suggest that a five Mega-pixel camera currently provides a realistic resolution entry point for routine surface measurement. It is essential to model radial lens distortion; uncompensated radial distortion errors effectively constrain the accuracies achievable. It is hoped that a freely accessible web site maintained by the first named author can become a useful repository for camera calibration data for medium accuracy surface measurement.

ACKNOWLEDGEMENTS

The tests conducted in this study used the IMAGINE OrthoBASE Pro software package distributed by Leica Geosystems. Initial tests were carried out using OrthoBASE Pro version 8.6 but results were verified using LPS 8.7. It is expected that LPS version 8.8 will provide appropriate camera calibration capabilities for consumer grade digital cameras and the authors acknowledge the work of Dr Younian Wang and Mladen Stojic at Leica Geosystems in this respect. The authors also acknowledge the financial support provided by the Association of Commonwealth Universities and British Academy, which helped to support the collaboration between the first two authors. Finally, the supportive and

constructive suggestions made by two anonymous referees were found to be valuable.

REFERENCES

ABDEL-AZIZ, Y. I. and KARARA, H. M., 1971. Direct Linear Transformation from comparator coordinates into object space coordinates in close-range photogrammetry. *American Society of Photogrammetry, Symposium on Close-Range Photogrammetry*, Urbana, Illinois 433 pages: 1-18.

ATKINSON, K. B., 1996. *Close Range Photogrammetry and Machine Vision*, Whittles Publishing, Scotland, 384 pages: 166-168.

BROWN, D.C., 1972. Calibration of close range cameras, *XII Congress of the International Society of Photogrammetry*, Ottawa, 26 pages.

CARDENAL, J., MATA, E., CASTRO, P., DELGADO, J., HERNANDEZ, M. A., PEREZ, J. L., RAMOS, M. and TORRES, M., 2004. Evaluation of a digital non metric camera (Canon D30) for the photogrammetric recording of historical buildings, *International Archives of Photogrammetry, Remote Sensing ,and Spatial Information Science* 35(B5): 564-569.

CHANDLER J. H. and BRUNSDEN, D., 1995. Steady state behaviour of the Black Ven mudslide: the application of archival analytical photogrammetry to studies of landform change. *Earth Surface Processes and Landforms*, 20(3): 255-275.

CHANDLER, J. H. and CLARK, J. S., 1992. The archival photogrammetric technique: further application and development. *Photogrammetric Record*, 14(80): 241-247.

CHANDLER, J. H., SHIONO, K., RAMESHWAREN, P. and LANE, S. N., 2001. Measuring flume surfaces for hydraulics research using a Kodak DCS460. *Photogrammetric Record*, 17(97): 39-61.

CHANDLER, J. H., BUFFIN-BELANGER, T., RICE, S., REID, I. and GRAHAM, D. J., 2003. The accuracy of a river bed moulding/casting system and the effectiveness of a low-cost digital camera for recording river bed fabric, *Photogrammetric Record*, 18(103): 209-223.

DESMOND, L. G. and BRYAN, P. G., 2003. Recording architecture at the archaeological site of Uxmal, Mexico: A historical and contemporary view, *Photogrammetric Record*, 18(102): 105-130.

DPREVIEW, 2004. Nikon Coolpix 3100 digital camera specifications. http://www.dpreview.com/reviews/specs/Nikon/nikon_cp3100.asp. [Accessed, 3rd August, 2004].

EL-HAKIM, S. F., FRYER, J. G. and PICARD, M. 2004, Modelling and visualization of aboriginal rock art in the Baiame cave. *International Archives of Photogrammetry and Remote Sensing*, 35(B5): 990-995.

ERDAS, 2002. *Imagine OrthoBASE user's guide*. Leica Geosystems, Atlanta, 483 pages: 341.

FAIG, I. W., 1975. Calibration of close range photogrammetric systems. *Photogrammetric Engineering and Remote Sensing,* 41(12): 1479-1486.

FRASER, C. S. and SHORTIS, M. R., 1995. Metric exploitation of still video imagery. *Photogrammetric Record*, 15(85): 107-122.

FRASER, C.S., 1997. Digital camera self-calibration. ISPRS Journal of Photogrammetry and Remote Sensing, 52: 149-159.

FRYER, J. G., 1988, Camera Calibration, Non-Topographic Photogrammetry, (2nd Ed.), American Society of Photogrammetry, 40 pages.

FRYER, J. G., 2001, Surveyors and Archaeology: Recording Timeless Treasures, *Geomatics World*, 6(9): 24-27.

FRYER, J. G., and MITCHELL, H.L., 1987. Radial distortion and close-range stereo photogrammetry. *Australian journal of Geodesy, Photogrammetry and Surveying*, 46/47: 123-138.

GANCI, G. and SHORTIS, M.R., 1996. A comparison of the utility and efficiency of digital photogrammetry and industrial theodolite systems. *International Archives of Photogrammetry and Remote Sensing*, 31(B5): 182-187.

GOOCH, M. J. and CHANDLER, J. H., 1998. Optimization of strategy parameters used in automated Digital Elevation Model generation*, ISPRS International Archives of Photogrammetry and Remote Sensing*, 32(2): 88-95.

HANCOCK, G. and WILLGOOSE, G. 2001. The production of digital elevation models for experimental model landscapes. *Earth Surface Processes and Landforms* 26(5): 475-490.

HOTTIER, P., 1976. Accuracy of close-range analytical restitutions: practical experiments and predictions. *Photogrammetric Engineering and Remote Sensing,* 42(3): 345-375.

KENEFICK, J. F., HARP, B. F. and GYER, M. S., 1972. Analytical self-calibration. *Photogrammetric Engineering*, 38(11): 1117-1126.

LANE, S. N., JAMES, T. D. and CROWELL, M. D., 2000. Application of digital photogrammetry to complex topography for geomorphological research. *Photogrammetric Record,* 16(95): 793-821.

LAWLESS, M. and ROBERT, A. 2001. Three-dimensional flow structure around small-scale bedforms in a simulated gravel-bed environment. *Earth Surface Processes and Landforms*, 26(5): 507-522.

LI, Z. L., 1988. On the measure of digital terrain model accuracy. *Photogrammetric Record,* 12(72): 873-877.

MITCHELL, H.L. and NEWTON, I., 2002. Medical Photogrammetric Measurement: Overview and Prospects, *ISPRS Journal of Photogrammetry and Remote Sensing*, 56(5-6): 286-294.

OGELBY, C.L., 2004. Heritage documentation– the next 20 years. *International Archives of Photogrammetry, Remote Sensing ,and Spatial Information Science,* 35(B5): 855-860.

OGLEBY, C. L., PAPADAKI, H., ROBSON, S. and SHORTIS, M. R., 1999. Comparative camera calibrations of some "off the shelf" digital cameras suited to archaeological purposes. *International Archives of Photogrammetry and Remote Sensing,* 32(5W11): 69-75.

PATIAS, P. and STREILEIN, A., 1996. Contribution of videogrammetry to the architectural restitution results of the CIPA "O. Wagner Pavillion" test. *International Archives of Photogrammetry and Remote Sensing*, 31(B5): 457-462.

SHORTIS, M. R., ROBSON, S. and BEYER, H. A., 1998. Principal point behaviour and calibration parameter models for Kodak DCS cameras. *Photogrammetric Record,* 16(92): 165–186.

SKARLATOS, D., 1999. Orthophotograph production in urban areas. *Photogrammetric Record,* 16(94): 643-650.

STOJIC, M., CHANDLER, J., ASHMORE, P. and LUCE, J., 1998. The assessment of sediment transport rates by automated digital photogrammetry. *Photogrammetric Engineering and Remote Sensing,* 64(5): 387-395.

WALSTRA, J., CHANDLER, J. H., DIXON, N. and DIJKSTRA, T. A., 2004. Time for change– quantifying landslide evolution using historical aerial photographs and modern photogrammetric methods *International Archives of Photogrammetry and Remote Sensing,* 35(4)*: 474-480.*

WANG, Y., 2004. Personal communication.

ZHIZHUO, W., 1990. *Principles of photogrammetry*, Publishing House of Surveying and Mapping, Beijing, 575 pages: 183.

Résumé

Zusammenfassung

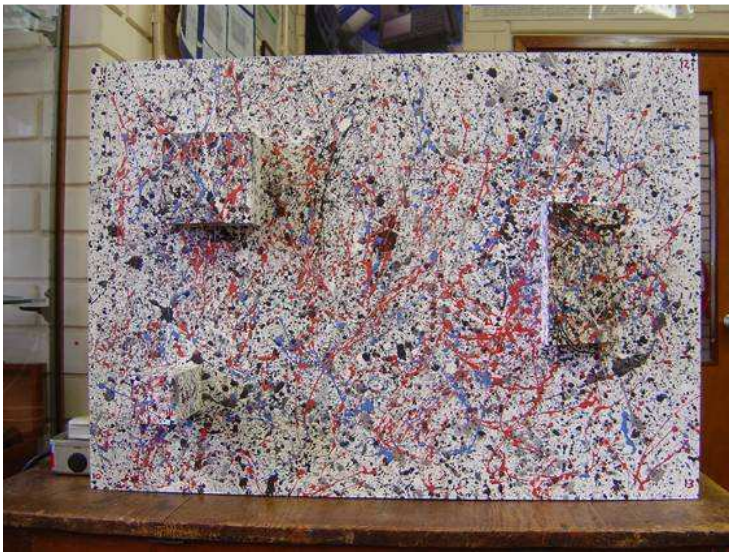

Figure 1- Test object (acquired using Sony DSC-P10)

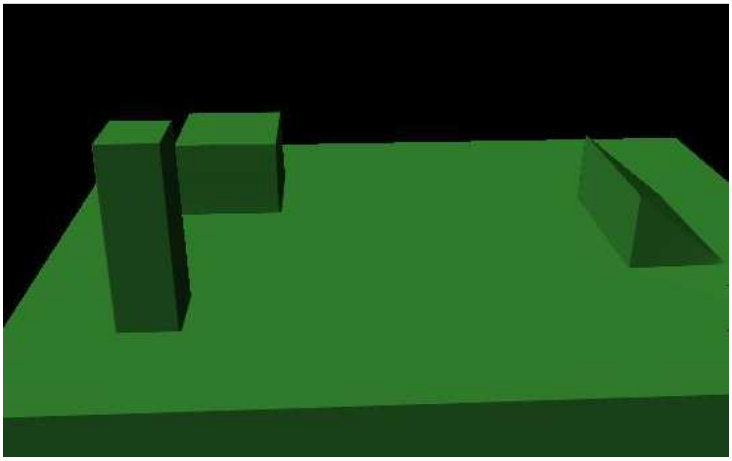

Figure 2- Rendered block model of "truth DEM", note slight vertical exaggeration

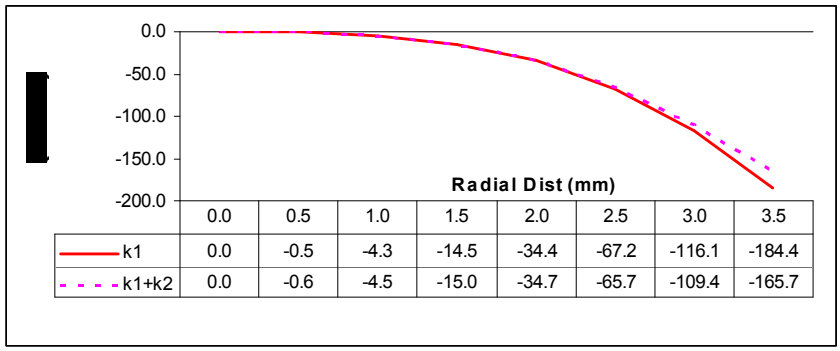

	0.0	0.5	1.0	1.5	2.0	2.5	3.0	3.5
k1	0.0	-0.5	-4.3	-14.5	-34.4	-67.2	-116.1	-184.4
k1+k2	0.0	-0.6	-4.5	-15.0	-34.7	-65.7	-109.4	-165.7

Figure 3- Number of parameters required to define radial lens distortion, Nikon Coolpix

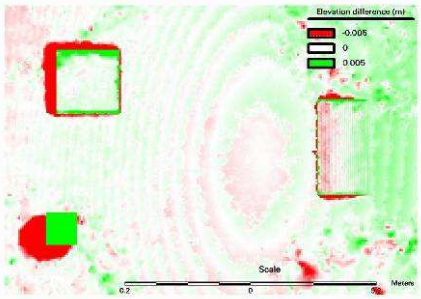

Figure 4- Elevation differences- Kodak DCS460

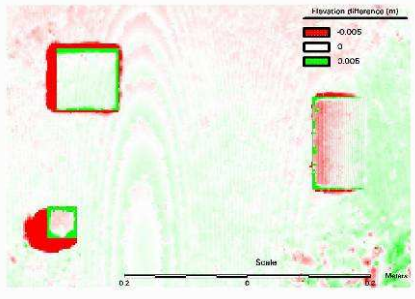

Figure 5- Elevation differences- Sony DSC-P10

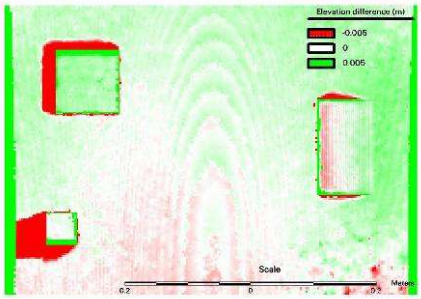

Figure 6- Elevation differences- Olympus C3030

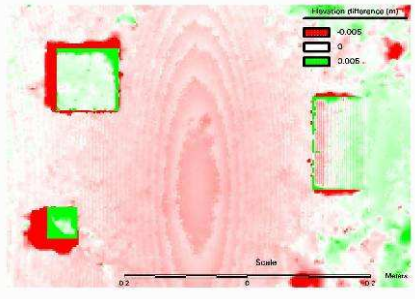

Figure 7- Elevation differences- Nikon Coolpix